New High Resolution Airborne Geophysical Surveys In Nevada And California For Geothermal And Mineral Resource Studies

Jonathan M.G. Glen and Tait E. Earney

U.S. Geological Survey, Moffett Field, CA 94035

Keywords

GeoDAWN, GeoFlight, aeromagnetics, aeroradiometrics, geophysics, geothermal resources, mineral resources, lithium, Nevada, California, Great Basin, Walker Lane, Salton Trough

ABSTRACT

The U.S. Geological Survey (USGS) and the Department of Energy (DOE) are collaborating to acquire high-resolution airborne magnetic and radiometric data to support geologic and geophysical mapping and modeling that will assist geothermal and critical mineral studies. Coordinated with these efforts are programs supporting geologic mapping and airborne lidar (light detection and ranging) surveys that yield detailed surface topographic models of the terrain over the same regions spanned by the geophysical surveys. The collaboration leverages resources from the USGS and DOE to acquire large regional datasets that will provide fundamental data necessary to map surface and subsurface geology and structure to benefit mineral and resource program objectives of both agencies. Such regionally uniform datasets are important for geothermal research to assist in identifying geologically favorable settings and as inputs in predictive models targeting undiscovered resources that use knowledge-driven (e.g., play fairway analysis) or data-driven approaches (e.g., machine-learning methods) to reduce risk associated with resource exploration. These data will also serve a wide range of other related activities from hazard (earthquake, volcano, landslide, environmental) and resource (water, mineral, energy) studies, to mapping and land management.

Surveys were conducted in two selected areas that host substantial geothermal and mineral potential in California and Nevada. The data will aid several ongoing USGS and DOE projects aimed at characterizing geothermal and mineral systems, understanding the factors controlling their occurrence, and improving future national resource assessments. The first of these surveys (referred to as GeoDAWN) was collected over northern and western Nevada and eastern California and spans areas of major resource potential associated with the Walker Lane and western Great Basin. This includes Clayton Valley, which hosts substantial lithium brine and clay resources, and the Humboldt mafic Complex, which constitutes a potentially important resource of critical minerals (including cobalt, rare earth elements, platinum group elements, iron, chromium, nickel, and copper). The second survey area (referred to as GeoFlight) is focused over the Salton Trough

in southern California that contains some of the largest and hottest known hydrothermal systems in the world, as well as a substantial lithium brine resource that could potentially meet the nation's lithium demand for electric vehicles. Data from both surveys will be made publicly available through USGS publications and online data repositories.

1. Introduction

The U.S. Geological Survey (USGS) and Department of Energy (DOE) are collaborating on efforts to collect extensive high-resolution airborne geophysical data in two regions of the western United States (Figure 1) that target areas with substantial potential for both critical minerals and geothermal resources. The surveys are being conducted under the USGS's Earth Mapping Resource Initiative (EarthMRI), with support from the DOE's Geothermal Technologies Office (GTO). The surveys involved acquisition of aeroradiometric and aeromagnetic data that provide key information on surface geology and soil composition, and subsurface structure and geology that are fundamental to a wide range of hazard (earthquake, volcano, landslide, environmental) and resource (water, mineral, energy) studies, and to mapping and land management efforts.

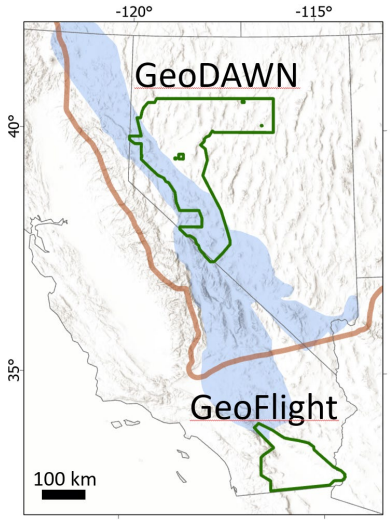

Figure 1. Regional index map showing the extent of GeoDAWN and GeoFlight surveys (green outlines). Blue colored region shows extent of Walker Lane (after Faulds and Henry, 2008). Brown line reflects boundary of the Great Basin (after Glen et al., 2022). Base map from the ArcGIS online map server (Esri, 2022).

These surveys are intended to directly support USGS and GTO missions to increase geothermal energy research, and aid exploration and development[1]. The surveys are fundamental for geothermal reservoir characterization because they provide high-resolution data capable of resolving detailed geology and structure that is essential to understanding controls on hydrothermal fluid flow. These uniform and regionally-extensive datasets, spanning numerous proven systems can be valuable inputs to predictive models targeting undiscovered resources that use knowledge-

[1] https://www.energy.gov/eere/geothermal/geothermal-technologies-office;
https://www.usgs.gov/centers/gmeg/science/geothermal-resource-investigations-project

driven (e.g., play fairway analysis) or data-driven approaches (e.g., machine-learning methods). They also offer the advantage that they can be used for both broad geologic mapping that provides regional context to deciphering local structure and geology, as well as for detailed site-specific studies of individual mineral or geothermal systems. In addition, these data can and are typically integrated with other datasets (e.g., gravity and electrical data) commonly used to characterize the subsurface.

The surveys will immediately benefit several ongoing DOE and USGS funded projects such as the GTO's Hidden Systems Initiative, aimed at discovery of hidden geothermal systems in the Basin and Range (Earney et al., 2022), and USGS efforts to develop new national geothermal resource assessments of conventional and enhanced geothermal systems (EGS) resources (Burns and Glen, 2023).

The surveys span numerous active and prospective energy and mineral resource areas, and include important areas of conventional moderate- to high-temperature hydrothermal resources, low-temperature and coproduced resources, and EGS. As such, the data could aid future geothermal exploration by helping to reduce overall risk and costs associated with geothermal drilling, and may help advance the commercial viability of EGS projects.

Part of the EarthMRI mission is to coordinate with State Geological Surveys to conduct new detailed geologic mapping focused on priority critical mineral targets within the survey extents[2]. EarthMRI also works with the USGS's 3D Elevation Program (3DEP) to collect airborne lidar (light detection and ranging) data over the same regions spanned by the geophysical surveys.

These two survey areas were prioritized because they carry important resource potential and represent regions where existing data are among some of the lowest quality in the country that are insufficient for satisfying advanced state-of the art mapping and modeling needs (Drenth and Grauch, 2019).

The first of the surveys (Geoscience Data Acquisition for Western Nevada project, GeoDAWN, Figure 2) was collected over northern and western Nevada and eastern California and spans areas of major resource potential associated with the Walker Lane and western Great Basin (Faulds et al., 2021). This includes Clayton Valley, which hosts substantial lithium brine and clay resources (Bradley_et al., 2017), and the Humboldt mafic Complex, which constitutes a potentially important resource of critical minerals (including cobalt, rare earth elements, platinum group elements, iron, chromium, nickel, and copper; Johnson and Barton, 2000).

The second survey area (referred to as GeoFlight, Figure 3) is focused over the Salton Trough in southern California that contains some of the largest and hottest known hydrothermal systems in the world (Hulen et al., 2002), as well as a lithium brine resource that could potentially produce half the current global lithium production (McKibben et al., 2021).

[2] https://www.usgs.gov/special-topics/earth-mri

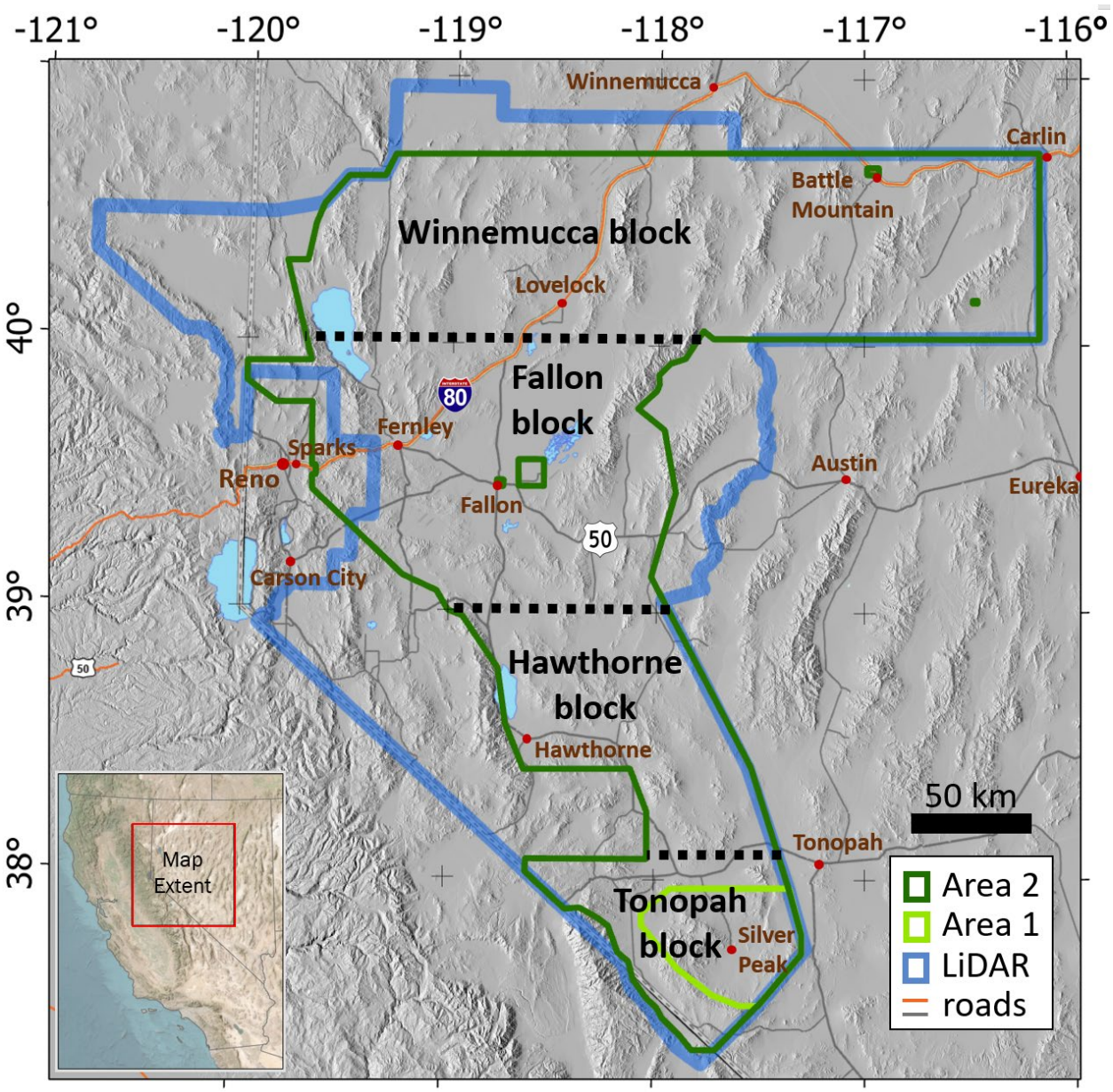

Figure 2. Index map of the GeoDAWN survey showing survey areas (green polygons), acquisition blocks (labeled and delineated by dashed black lines), extent of lidar collection (thick blue polygon). Base map from the ArcGIS online map server (Esri, 2022).

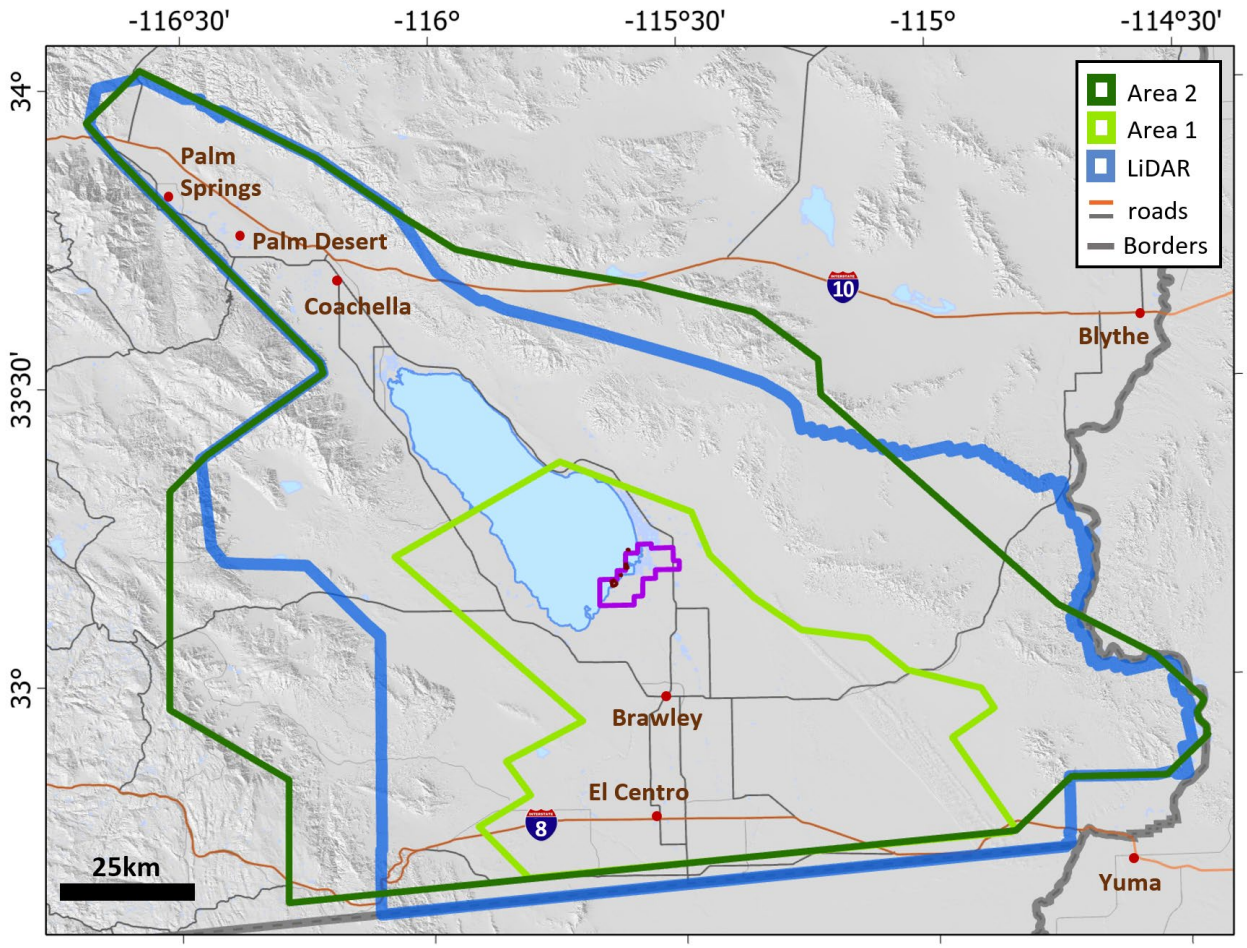

Figure 3. A) Index map of the GeoFlight survey showing the extent of lidar collection (blue polygon) relative to the GeoFlight survey areas (green polygons). Also shown is the extent of the Salton Sea Geothermal Field (SSGF, purple polygon). Base map from the ArcGIS online map server (Esri, 2022).

2. Data Acquisition

2.1 Radiometrics

Airborne radiometric methods are used to determine the natural radioactivity (gamma radiation) of radiogenic isotopes of potassium, uranium and thorium from near-surface rocks and soils using a gamma ray spectrometer installed on the aircraft. Gamma radiation from these elements can be distinguished by their characteristic energy, allowing one to measure the contributions from these different radioelements. The data are subject to standard methods to correct for radon, aircraft and cosmic background radiation, Compton scattering, and height attenuation (Erdi-Krausz et al., 2003). The resulting processed measurements reveal information on the concentrations of radioactive isotopes of potassium (^{40}K), uranium (^{238}U), and thorium (^{232}Th) in the upper ~1/2 m of the ground surface.

Because gamma-rays are highly penetrating, and can travel several tens of centimeters through rock and several hundred meters through the air, radiometric measurements can be conducted from airborne platforms (drone or manned aircraft). However, attenuation of the radiometric signal with

distance from the source limits the method's effectiveness to within several hundred meters of the ground surface.

Distinct radionuclide concentrations or their ratios can be used to distinguish variations in lithology and soil, and to identify areas of alteration and weathering (Duval. 1989). As gamma rays are emitted upon decay of ^{40}K to argon, potassium abundance can be measured directly. However, ^{232}Th and ^{238}U concentrations are determined from the gamma radiation of their decay products and are based on the assumption of equilibrium of their decay series. As a result, ^{232}Th and ^{238}U concentrations are referred to as "equivalent" concentrations (Erdi-Krausz et al., 2003). A standard way of representing ground radiometric concentrations is in units of percent for K, and parts per million (ppm) for Th and U, because K is more prevalent in the Earth's crust. Radiometric data are also commonly portrayed in maps of ratios (eU/eTh, eTh/K and eU/K), or as a ternary map (Duval, 1983) that depicts radiometric abundances in a three-color (red, green, and blue) composite grid.

These elements form large positive ions in minerals with crystal structure that can accommodate them. They occur in various concentrations in different rock types and their weathering products, thus these data can provide an important tool for mapping surface geology and soil, provided there is sufficient understanding of a setting's rock and soil geochemistry, and of the processes that effect the distribution and mobility of the radioelements.

Potassium is commonly found in feldspars (e.g., K-feldspar, microcline, orthoclase) and micas (e.g., muscovite and biotite). Uranium and thorium commonly occur in accessory minerals such as apatite, sphene and zircon in igneous and metamorphic rocks, and tend to be more prevalent in felsic rocks and to increase with alkalinity (Hoover et al., 1992). Granitoids and metasediments are commonly associated with particularly high K concentrations, as well as enhanced U and Th. Shales commonly contain clay minerals that can accommodate K, U, and Th in their crystal structure, as wells as K found in grains of mica and feldspar. Sandstones and conglomerates can, in addition to containing any primary grains or clasts hosting radioactive minerals, acquire radioelements post deposition by way of groundwater or hydrothermal circulation. Metamorphic rocks derived from parent rocks that have high contents of radioactive elements can retain their parent radioelement chemistry.

In places where weathering products are largely in situ, they often reflect underlying lithology. In this case, aeroradiometric data collected over covered areas may still be used to characterize bedrock geology. Nonetheless, the nature of the overburden can dramatically change the radiometric signal from the parent bedrock through alteration and conditions such as soil moisture, thickness of soil, and geometry of the source, which can decrease radiation from the underlying bedrock. Ground cover can dramatically attenuate the surface radiometric signal and may preclude the use of the method over areas where water, snow, permafrost, or vegetation are present (Erdi-Krausz et al., 2003).

Although U is chemically active across a range of temperatures and pH, and is therefore relatively mobile in groundwater, Th, being much less soluble than U (and K), is relatively stable. As a result, different types of chemical and physical alteration can lead to distinct changes in the concentration of these isotopes from the parent rock geochemistry. U/Th ratios can be sensitive to conditions during diagenesis, deformation, or hydrothermal alteration, due to, for example,

enhancement of U relative to Th under reducing conditions, or depletion of U relative to Th under oxidizing conditions (Airo, 2002).

Because K is the most abundant of the three radioelements in most bedrock, alteration is often manifest as prominent shifts in K concentrations and can be used to identify alteration zones. On the contrary, U and Th are commonly enhanced in metasedimentary rocks, where they can mask the role of K.

Hydrothermal alteration can lead to changes in the U, Th, and particularly K content of rocks that can aid mineral exploration. Elevated concentrations of K in mafic to ultramafic rocks, that typically lack K bearing minerals may indicate potential targets for hydrothermal ore mineralization that has resulted in K enrichment (Airo, 2002).

Hydrothermal alteration associated with gold mineralization is commonly accompanied by an increase in potassium, whereas decreases in U and Th are characteristic of hydrothermal alteration and magmatic intrusions (Maden and Akaryali, 2015).

2.2 Magnetics

In contrast to radiometric methods that help constrain surface geology and soil composition, magnetics provide information on the subsurface that is often difficult, time consuming, and expensive to derive by other means. This is especially important in areas where bedrock may be concealed, like the Basin and Range that is largely covered by young sediments and volcanics[3].

Magnetic data reveal subtle fluctuations in the magnetic field that reflect variations in magnetization of rocks in the subsurface. These datasets can be used in mapping and modeling subsurface geologic structures such as faults and contacts that juxtapose rock types with markedly contrasting magnetic properties (magnetic susceptibility and remanent magnetization), resulting in distinct magnetic anomalies that can help resolve the geometry and origin of buried sources. As a result, magnetic data can be put to a variety of applications that span mapping, hazards (earthquake, volcano, landslide), environmental, and resource (energy, mineral, water) studies.

Magnetic methods are used in geothermal exploration to facilitate imaging of subsurface structures. They are applicable to virtually all aspects of geothermal resource studies, but are most commonly deployed to studies of conventional hydrothermal systems that rely on natural, structural permeability, where they are used to map subsurface geology and structure (fault/fracture/contacts that may provide pathways or barriers to fluid flow), model reservoir geometries, and map hydrothermal alteration. Mapping structure, however, is also relevant to EGS studies, due to the need to characterize structures to properly manage an EGS resource (e.g., to mitigate fluid loss and triggered seismicity that may involve nearby existing structures).

A rock's magnetization commonly consists of both induced and remanent magnetization components and depends on the content and composition of its constituent magnetic minerals. Mafic to ultramafic rocks generally have strong magnetizations because they typically contain more strongly magnetic minerals such as magnetite (Carmichael, 1982). Relatively low average magnetizations are often associated with sedimentary and felsic igneous and metamorphic rocks.

[3]e.g., Cenozoic sediments cover 64% and 63% of the surface of GeoDAWN and GeoFlight extents, respectively.

In terrain with strongly magnetic mafic igneous rocks, remanence can dominate a rock's magnetization. In these situations, knowledge of the remanent components of magnetization can aid in interpretation and modeling magnetic anomalies.

Generally, gravity and magnetic highs arise from mafic and ultramafic igneous and crystalline basement rocks, whereas lows arise from felsic igneous, sedimentary, or altered basement rocks. Metamorphism and alteration can strongly affect the susceptibility of an originally homogeneous rock body by leading to the nonuniform production or destruction of magnetic minerals. Igneous outcrops not associated with magnetic anomalies might be thin or contain low concentrations of primary magnetic minerals or might have lost them due to alteration.

Some general conclusions can be drawn from the character of geophysical anomalies and their likely sources. The shallower the depth to a potential field source body, the higher the amplitude, the shorter the wavelength, and the steeper the gradients of its potential field anomaly. As a result, high-amplitude, short wavelength anomalies, which often have steep gradients, are produced by sources at shallow depths in the crust. In contrast, long-wavelength anomalies having smooth, low gradients commonly reflect deep sources. Anomalies with wavelengths of hundreds of kilometers, for example, most likely arise from sources in the lower crust. Although wide, shallow, thin sources with gently sloping sides can produce similar anomalies, such cases can usually be recognized with regional geologic mapping.

The size, geometry, and depth to a potential field source; the character of the geomagnetic field; and the rock properties of a source and its surroundings all determine the character of a source's anomaly. Despite this complexity, and the inherent nonunique nature of potential field model solutions, magnetic data can provide concrete constraints on the geometry and, inferentially, the origin of anomaly sources, particularly when combined with other constraints such as rock-property measurements, gravity, geology (regional tectonic framework, geologic mapping, drillcore and borehole geophysical logs, etc.), and seismic or electrical data.

Typically, a variety of derivative and filtering methods are applied to magnetic data to help: simplify anomalies to aid interpretations, delineate structures such as faults or contacts by resolving the edges source bodies, determine the depth and geometry of buried sources, and constrain sense and magnitude of offsets on faults. Residual maps, produced by upward-continuing the observed anomalies and subtracting the result from the original grid, can be used to remove the contribution of deeper sources, and emphasize surface and near-surface sources. The pseudogravity (or magnetic potential) transformation (Blakely, 1995), converts a magnetic anomaly into one that would be observed if the magnetic distribution of the body were replaced by an identical density distribution. Although there are significant assumptions that can limit its effectiveness, this method can be used to simplify the interpretation of magnetic sources by centering magnetic anomalies over their sources. Maximum horizontal gradients (MHG; Blakely and Simpson, 1986) of pseudogravity, which reflect abrupt lateral changes in the magnetization in the subsurface, and tend to lie over the edges of bodies with near vertical boundaries, are used to estimate the extent of buried sources (Grauch and Cordell, 1987; Cordell and McCafferty, 1989). 2D and 3D modeling are typically employed to constrain 3D structural geometry, and provide a structural basis for subsequent 3D geologic, stress and hydrologic models.

Several factors can influence a rock's magnetic mineralogy (and hence its magnetization) throughout its lifetime. Hydrothermal alteration often results in the destruction of magnetite and

can progressively reduce the primary magnetization of the host rock (Bouligand et al., 2014). Under these conditions, the magnitude of the anomaly associated with alteration will reflect the intensity and duration of alteration processes and may indicate how long-lived a current or fossil hydrothermal system may have been active. However, under some conditions, such as serpentinization or potassic alteration (Clark, 1997) secondary magnetite may also be produced. As a result, a rock's history and potential processes that may have altered the magnetic properties of the parent material should be considered.

3. Surveys

The GeoDAWN and GeoFlight airborne geophysical surveys (Figures 1-3) provide broad, uniformly distributed datasets that will help constrain surface and subsurface geology and structure. They were designed to yield high-resolution data sufficient for 3D-characterization of magnetic anomaly sources. Both areas were selected (with input from several participating collaborators[4]), based on a variety of factors. The principal aim was to collect data in priority areas (based on GTO and USGS objectives) with substantial critical mineral and geothermal potential that lacked the requisite framework geoscience data (geologic mapping, geophysical surveys, and lidar data) for detailed state-of the art geologic and geophysical studies. A key factor in defining the surveys extents was the existing available aeromagnetic data. For both areas the existing aeromagnetic coverage represents a patchwork compilation of variable quality[5] data consisting of mostly low-resolution[6] surveys (Figures 4-5) that are generally not suitable for quantitative analyses, and in many cases are of little or no utility for robust geologic interpretation. An important consideration was also to balance the need of collecting data over as large of an area as possible[7] (with existing funding), while maintaining requisite high quality data standards.

[4]The GeoDAWN and GeoFlight surveys were planned and conducted with input from a number of participating groups including: Federal Emergency Management Agency, US Department of Agriculture, Natural Resources Conservation Service, Bureau of Land Management, US Bureau of Reclamation, Nevada Bureau of Mines and Geology, California Geological Survey, California Energy Commission, Department of Defense -Navy Geothermal Program Office, USGS Earthquake Hazards Program, and Tribal Nations.

[5]Survey quality (Drenth and Grouch, 2019) is defined by a variety of factors including flight height, flightline spacing, whether the original digital data are available or the survey was digitized from published maps, and aircraft positioning error (which relates to whether positioning was pre- or post-GPS availability).

[6] https://mrdata.usgs.gov/airborne/map-us.html

[7]A large area is critical to predictive models targeting undiscovered resources that use data-driven machine-learning approaches, because it is more likely to encompass numerous known systems that can be used as training sites for models.

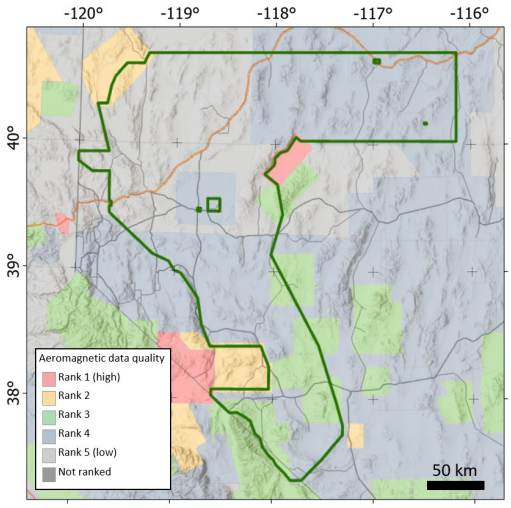

Figure 4. Index map depicting existing aeromagnetic coverage quality (https://mrdata.usgs.gov/airborne/map-us.html#home) across the GeoDAWN survey extent. Physiographic base maps from the ArcGIS online map server (Esri, 2022).

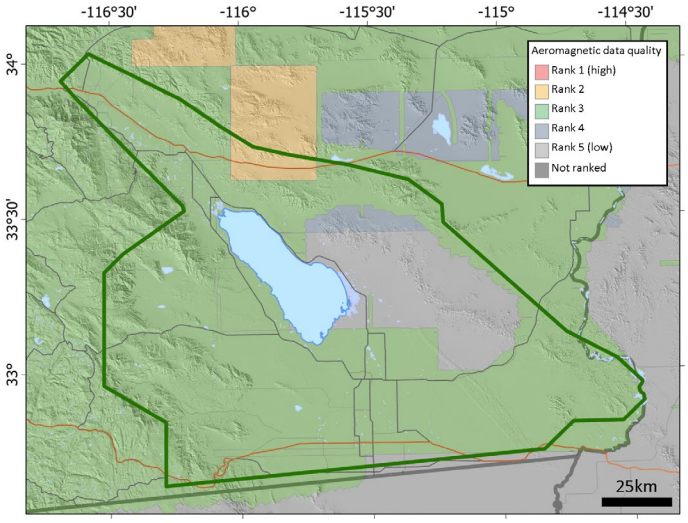

Figure 5. Index map depicting existing aeromagnetic coverage quality (https://mrdata.usgs.gov/airborne/map-us.html#home) across the GeoFlight survey extent. Physiographic base maps from the ArcGIS online map server (Esri, 2022).

3.1 GeoDAWN

High-resolution airborne magnetic and radiometric surveys over northern and western Nevada and eastern California were conducted by EDCON-PRJ, Inc., under contract with the USGS from November 1, 2021 to November 20, 2022. The surveys, referred to collectively as GeoDAWN, consisted of two different, overlapping surveys with different flight specifications (Area 1 and Area 2) that together span parts of the Walker Lane and northwestern Great Basin (Figures 1, 2).

The Great Basin is a region that has experienced substantial crustal thinning and is characterized by elevated heat flow. Several studies (e.g., Faulds et al., 2012) identify the western Great Basin and adjacent Walker Lane as quite favorable for hosting considerable undiscovered geothermal resources (in addition to hosting several known, well-characterized developed systems). The region is also known for its gold, copper, and critical mineral resources. This includes two mineral focus areas that support EarthMRI objectives related to critical minerals in the Clayton Valley area in western Nevada (Area 1, Figure 2), which carries substantial Li-clay and brine resources, and the Humboldt mafic complex in northern Nevada that has potential for hosting cobalt, nickel, chromium, and possibly rare earth elements (REEs) and platinum group elements (PGEs).

Area 1, centered over Clayton Valley was selected primarily with a focus on the region's lithium resources, to address EarthMRI objectives (Figure 1). It was flown with rank 1 specifications (following criteria outlined by Drenth and Grauch, 2019) that met EarthMRI survey requirements. Area 2, consisting of the remainder of the GeoDAWN extent, was selected primarily with a focus on geothermal resources (Figure 1). Lower resolution flight specifications designated for Area 2 (falling between rank 1 and 2) enabled data collection across a substantially larger area (spanning numerous known, prospective, and undiscovered geothermal and mineral systems) than would have been possible with rank 1 specifications.

The combined GeoDAWN area (consisting of a total of 149,030 line-km spanning an area of 51,857 sq km), was divided into four separate acquisition blocks (from north to south: Winnemucca, Fallon, Hawthorne, and Tonopah; Figure 2). The Tonopah block, which includes Area 1 and the southern part of Area 2 surveys, was flow by Precision GeoSurveys Inc. (under subcontract to EDCON-PRJ, Inc.), with a Bell Jet Ranger helicopter.

Area 1 was flown with a nominal flight height targeted at 100 m above terrain over low-relief areas and 150 m over mountainous areas. Flight lines were spaced 200 m apart at an azimuth of 90 degrees, and tie lines were spaced 2000 m apart at an azimuth of 180 degrees.

Area 2 was flow at a nominal flight height targeted at 150 m above terrain over low-relief areas and 200 m over mountain ranges. The survey was flown with flight lines spaced 400 m apart at an azimuth of 90 degrees, and tie lines spaced 4000 m apart at an azimuth of 180 degrees. The portion of Area 2 contained within the Tonopah acquisition block was flown with the Precision GeoSurveys' Bell Jet Ranger, while the remainder was collected by Cloudstreet Flying Service (under subcontract to EDCON-PRJ, Inc.) and flown with a Cessna 180 and Turbo 206 fixed-wing aircraft.

Nominal flight heights for both surveys were based on a best fit, pre-planned, three-dimensional draped surface designed with a maximum 22-degree climb/descent angle to follow terrain as closely as possible while maintaining a safe survey. Actual flight heights were subject to aircraft climb and descent limitations. In areas of steep terrain, the aircraft may have required deviating from the planned drape surface, and therefore variable terrain clearance should be considered when modeling and interpreting these data.

Magnetic data were processed by EDCON-PRJ, Inc. and include corrections for diurnal variations of the Earth's magnetic field, magnetic field of the aircraft, tie-line leveling, micro-leveling, and an International Geomagnetic Reference of the Earth for the time of the survey. Radiometric data

were processed by the contractor and include corrections for aircraft and cosmic background radiation, radon background, Compton scattering effects, and variations in altitude.

A grid of the total magnetic intensity anomaly (TMI) across the full extent of the GeoDAWN survey is shown in Figure 6. Prominent regional features include the Northern Nevada Rifts (Glen and Ponce, 2002; Ponce and Glen 2002, 2008) that form large, long wavelength, north-northwest trending magnetic highs extending across the northeastern part of the survey that reflect mid-Miocene mafic dike swarms, as well as a dominant northwest trending grain of high amplitude and high frequency anomalies associated with a wide range of lithologies (Mesozoic granites, Paleozoic strata, and late Tertiary volcanic rocks) within the Walker Lane (Glen et al., 2004). Locally the GeoDAWN data reveal structural detail lacking in existing data (Figure 7). Young basin faults recently mapped from lidar data near Battle Mountain displace weakly magnetic basin fill that produce subtle magnetic anomalies seen in ground magnetic data, and in the airborne GeoDAWN data (Figure 8). An example of GeoDAWN aeroradiometric data over the Fish Creek Mountains (Figure 9) reveals a close correlation of potassium concentrations with mapped geologic boundaries and also indicate prominent variations within units previously mapped as a single unit. These examples indicate these data can enhance efforts to map and model surface and subsurface geology and structure.

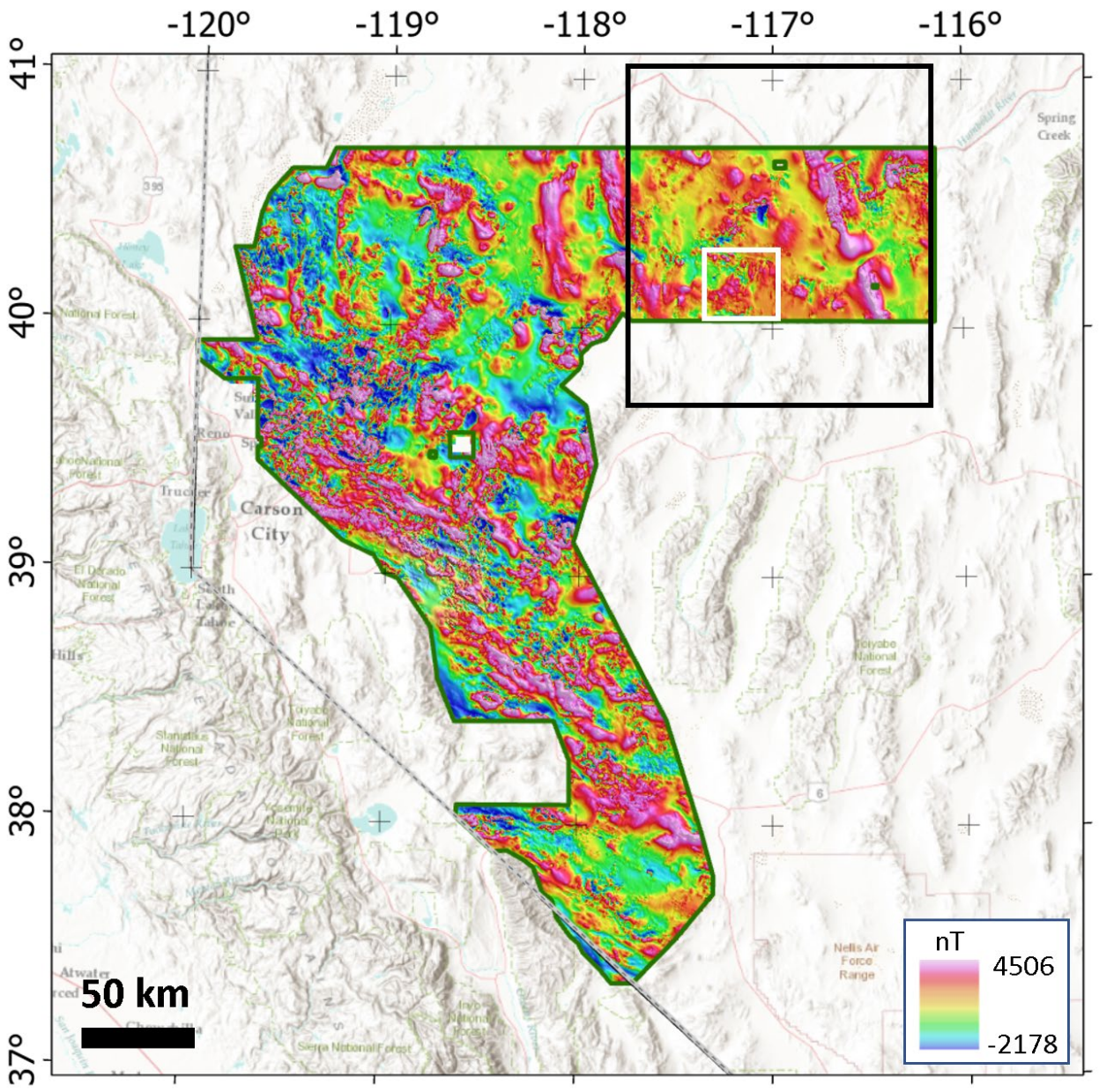

Figure 6. Shaded TMI map of the GeoDAWN survey in nanoteslas (nT). Black rectangle shows the extent of Figure 7. White rectangle shows the extent of Figure 9. Base map from the ArcGIS online map server (Esri, 2022).

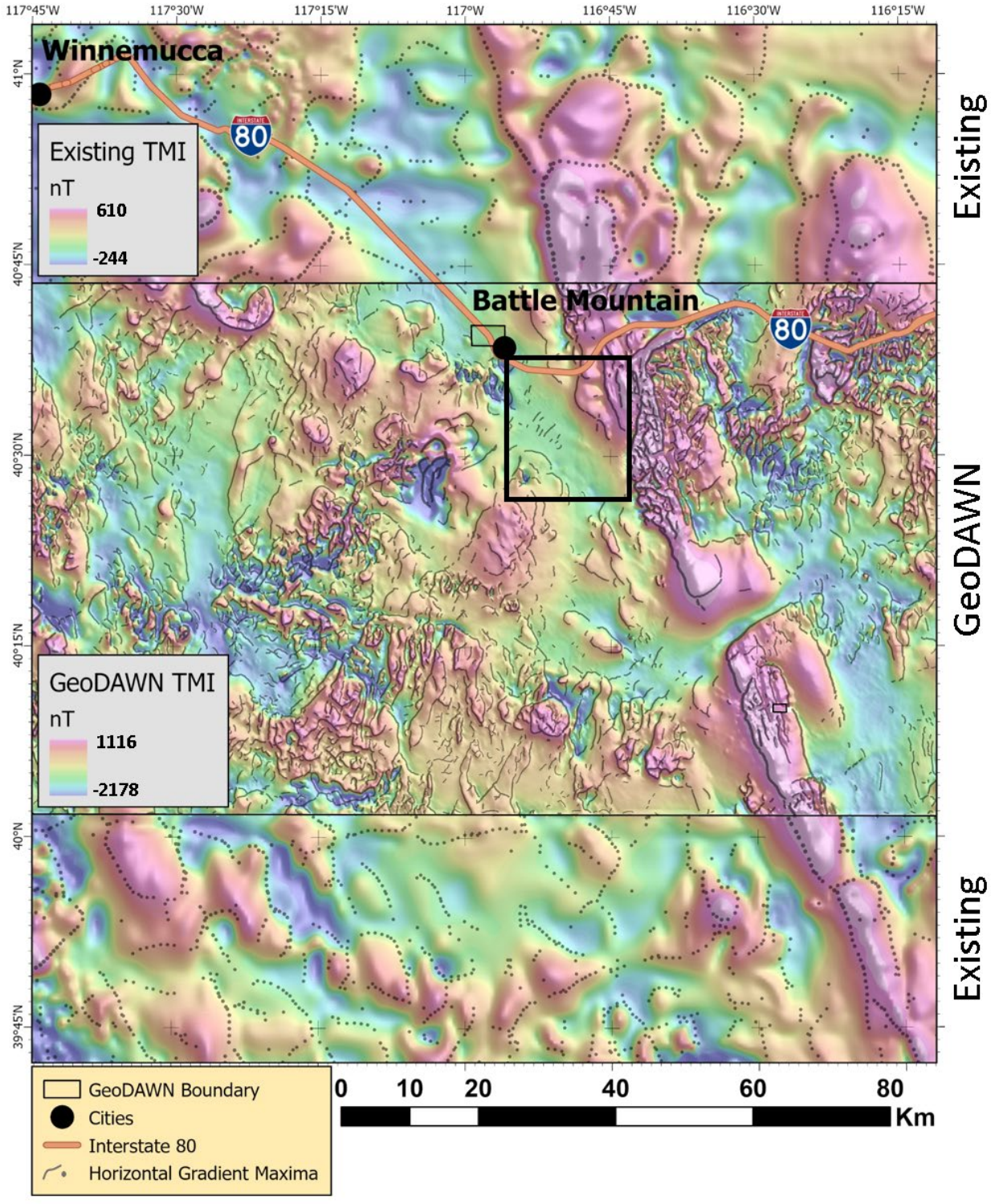

Figure 7. Shaded TMI (nanoteslas) map of the GeoDAWN survey (central portion) overlain on existing data from the state aeromagnetic compilation (Kucks et al., 2006) depicted at the top and bottom of the map. Superimposed on the map are points of maximum horizontal gradient that reflect abrupt lateral changes in the magnetization and are used to infer geologic structure. Extent shown in Figure 6. Black rectangle gives the extent of Figure 8. Base map from the ArcGIS online map server (Esri, 2022).

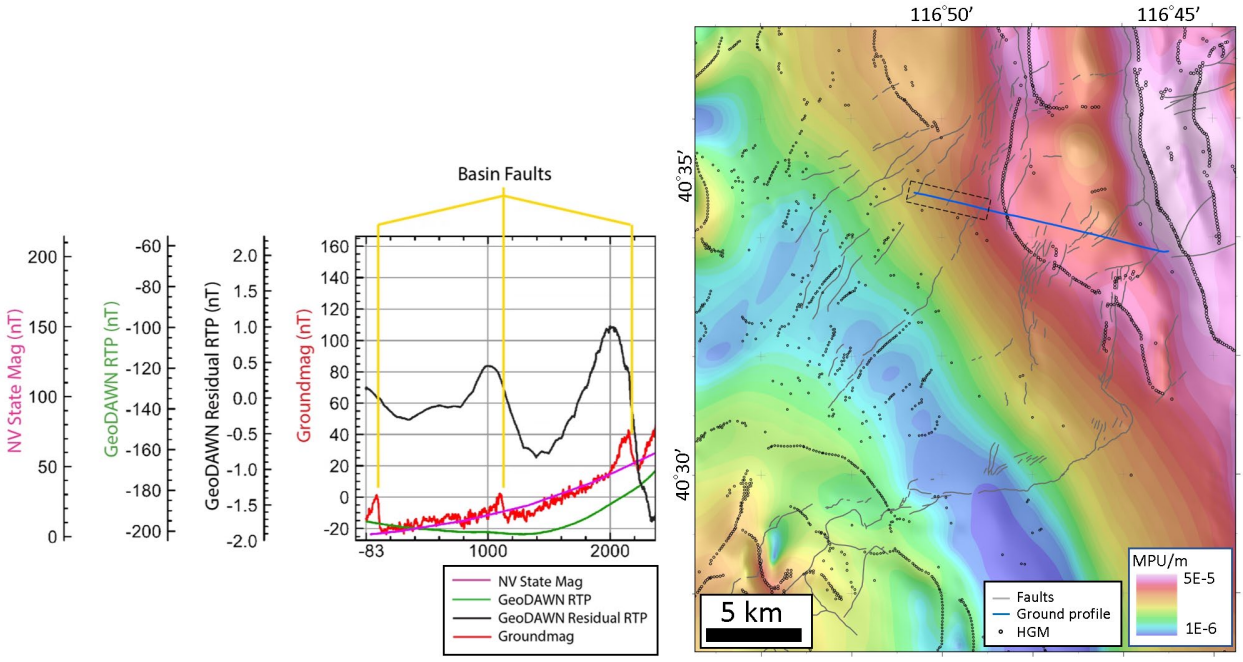

Figure 8. (Right) shaded horizontal gradient map of pseudogravity (in magnetic potential units per meter, MPU/m) of the GeoDAWN survey spanning the western margin of the northern Shoshone Range. Superimposed on the map are points of maximum horizontal gradient. Grey lines indicate recently mapped faults from lidar. (Left) graph comparing ground magnetic profile with GeoDAWN and existing aeromagnetic data along portion of profile (blue line) outline by dashed box on map. Also shown is a residual signal of the GeoDAWN data (after removing a regional signal) that reveals subtle anomalies associated with young basin faults that displace weakly magnetic basin fill. Extent shown in Figure 7. Base map from the ArcGIS online map server (Esri, 2022).

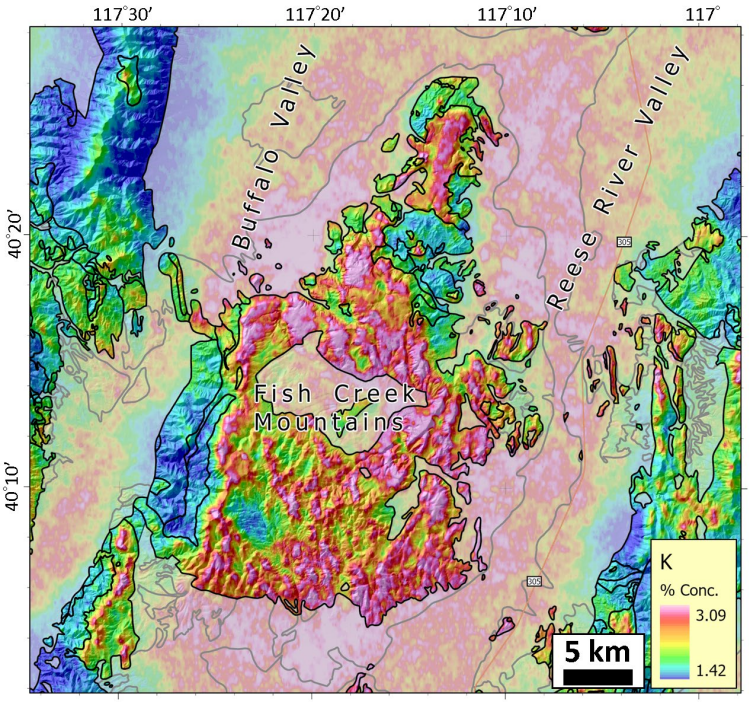

Figure 9. Shaded topographic map overlain by a grid of potassium concentrations from GeoDAWN aeroradiometric data over the Fish Creek Mountains (extent of map is shown on Figure 6 as a white box). Existing mapped geologic contacts are outlined in black. Geologic contacts are after Crafford (2007). Base map from the ArcGIS online map server (Esri, 2022).

3.2 GeoFlight

High-resolution airborne magnetic and radiometric surveys over southern California were conducted by EDCON-PRJ, Inc., under contract with the USGS from January 14, 2022 to March 26, 2023. The surveys, referred to collectively as GeoFlight, were situated over the Salton Trough and surrounding ranges, and largely centered on the Salton Sea geothermal field situated at the southern end of the Salton Sea.

A principal aim of these surveys is on lithium brine and geothermal resources (and their potential for co-production). However, it is also an important focus for Earthquake and Volcano Hazard Programs within the USGS because this area hosts some of the youngest volcanoes in the state and a segment of the San Andreas Fault (along the Coachella Valley) that carries potential for hosting a major earthquake (7-7.9)[8].

The GeoFlight surveys consisted of two different overlapping surveys flown with different aircraft (Areas 1 and 2, Figure 3). The combined GeoFlight surveys included a total of 94,671 line-km spanning an area of 16,772 sq km. Area 1 is centered on the Imperial Valley, and characterized by little topographic relief. The Area 1 survey was conducted by Precision GeoSurveys Inc. (under subcontract to EDCON-PRJ, Inc.), with a standard C-206 aircraft and flown with rank 1 specifications (Drenth and Grauch, 2019) that met EarthMRI survey requirements.

[8] https://www.usgs.gov/volcanoes/salton-buttes; https://www.usgs.gov/programs/earthquake-hazards/science/salton-seismic-imaging

Area 2, consisting of the remainder of the GeoFlight extent, was collected around the perimeter of Area 1 and included the most rugged topography across the entire region. Somewhat lower resolution flight specifications designated for Area 2 (falling between rank 1 and 2) were necessary for flight safety considerations over steep terrain, and also enabled data collection across a substantially larger area than would have been possible with rank 1 specifications that would otherwise have required acquisition by a helicopter. The Area 2 survey was conducted by Cloudstreet Flying Service (under subcontract to EDCON-PRJ, Inc.) with C-180 and Turbo C-206 aircraft.

The surveys were flown with flight lines spaced 200 m apart at an azimuth of 45 degrees, and tie lines spaced 2000 m apart at an azimuth of 135 degrees. Nominal flight heights were based on a best fit, pre-planned, three-dimensional draped surface designed with a maximum 20° climb/descent angle to follow terrain as closely as possible while maintaining a safe survey. This incorporated a variable terrain clearance of 120 m over low relief, 200 m over steep terrain, and 150 m over population centers. Actual flight heights were subject to aircraft climb and descent limitations. In areas of steep terrain, the aircraft may have required deviating from the planned drape surface, and therefore variable terrain clearance should be considered when modeling and interpreting these data.

Magnetic data were processed by EDCON-PRJ, Inc. and include corrections for diurnal variations of the Earth's magnetic field, magnetic field of the aircraft, tie-line leveling, micro-leveling, and an International Geomagnetic Reference of the Earth for the time of the survey. Radiometric data were processed by the contractor and include corrections for aircraft and cosmic background radiation, radon background, Compton scattering effects, and variations in altitude.

A grid of the TMI across the full extent of the GeoFlight survey is shown in Figure 10. Prominent regional features include high amplitude and high frequency magnetic highs in the Little San Bernardino, Chocolate, and Cargo Muchacho Mountains along the eastern extent of the survey over exposed bedrock. A series of prominent narrow magnetic highs and lows along the western edge of these ranges reflect strands of the southern San Andreas Fault zone that are not discernable in existing aeromagnetic data (Figure 11). Several long wavelength anomalies in the central part of the survey that occur along the axis of the basin reflect strongly magnetic buried sources. Magnetic data highlighting two of these features straddling the southern Salton Sea and Salton Sea geothermal field (SSGF) (Figure 12) reveal large, long wavelength circular anomalies (one situated over the Salton Buttes field and the other located entirely offshore) as well as several smaller high frequency features quite similar in character to the anomalies associated with the Buttes. These features likely reflect buried volcanic vents, flows and intrusives. Because the Buttes represent some of the youngest volcanics in the state, spatially and geophysically-similar anomalies may reflect an important source of shallow magmatism contributing heat and driving hydrothermal circulation in this area.

Several other examples from throughout the survey extent (Figure 13) reveal prominent anomalies associated with mapped faults that indicate the faults continue well beyond their mapped extent. There are numerous cases where the data reveal structures where none were previously mapped (with some of these correlating with zones of mineralization and active hydrothermal features).

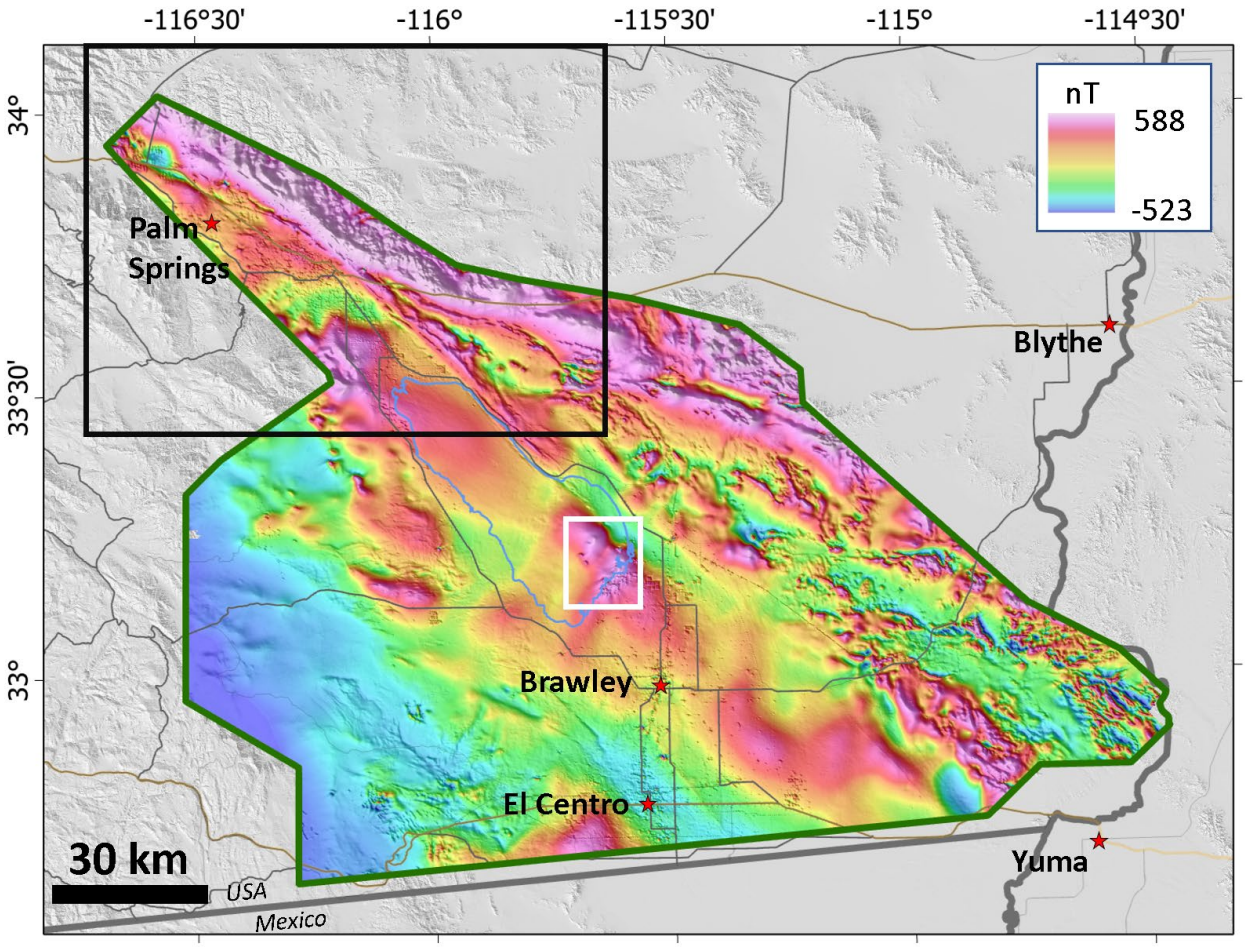

Figure 10. Shaded TMI (nanoteslas) map of the GeoFlight survey. Black rectangle shows the extent of Figure 11. White rectangle shows the extent of Figure 12. Faults are shown as black lines. Outline of the Salton Sea is shown with a light blue polygon. Base map from the ArcGIS online map server (Esri, 2022).

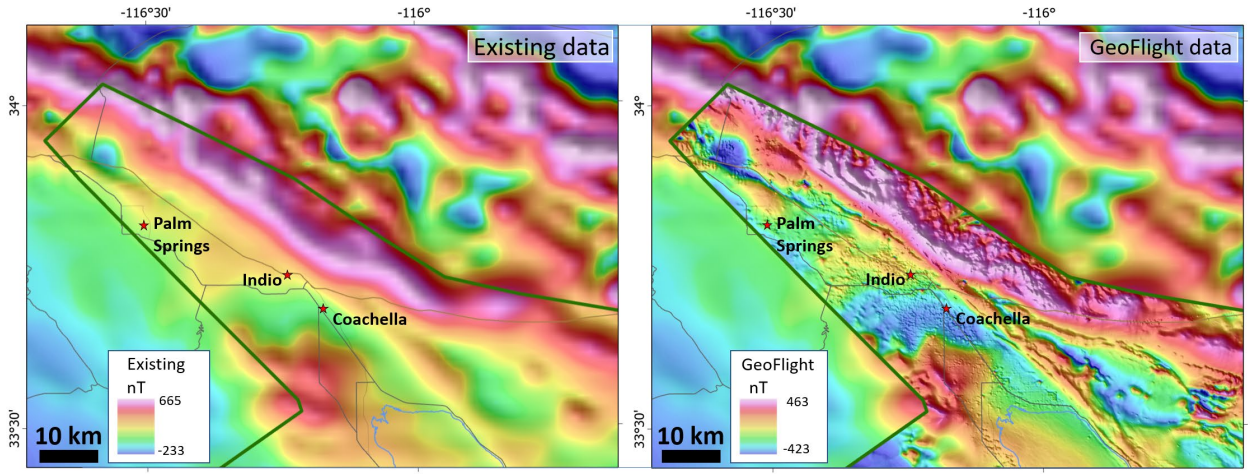

Figure 11. (Left) shaded TMI map of existing aeromagnetic data (Bankey et al., 2002), with GeoFlight data superimposed (right). Extent of map is shown on Figure 10 (as a black rectangle). Roads are shown as grey lines. Base maps from the ArcGIS online map server (Esri, 2022).

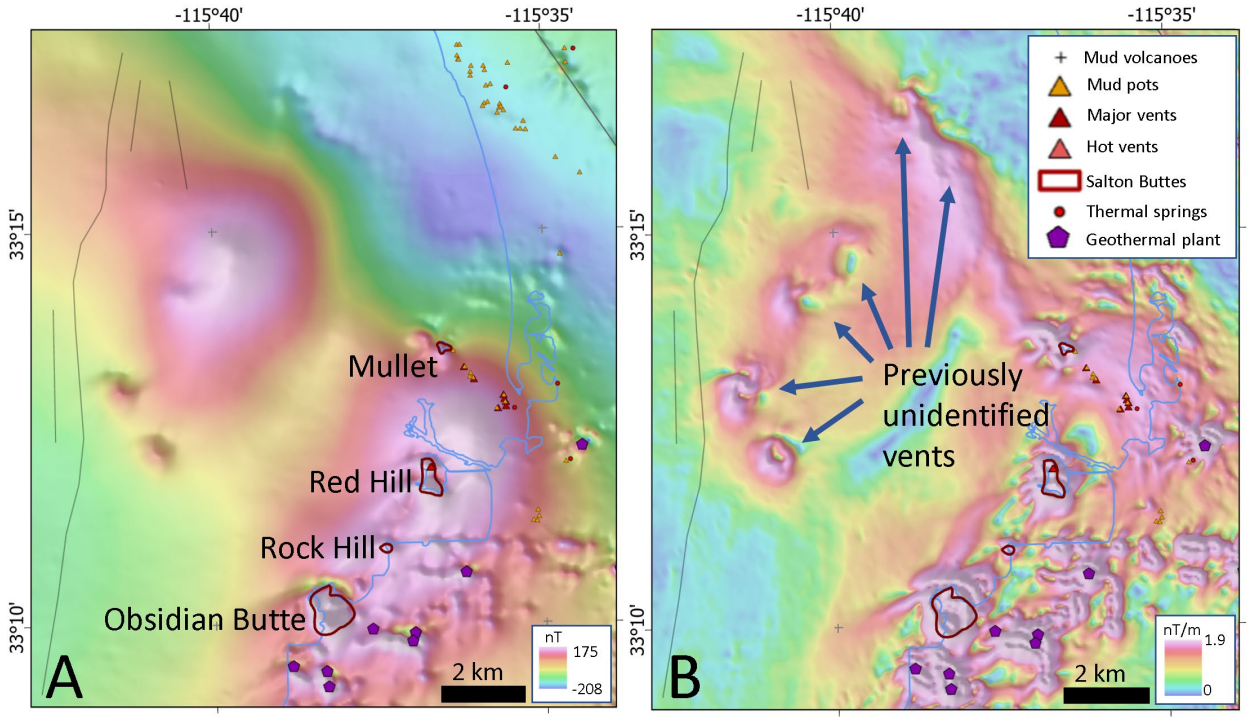

Figure 12. A) Shaded TMI map of GeoFlight data over the southern Salton Sea and Salton Sea geothermal field showing various geothermal features, volcanic buttes, and interpretive offshore features. B) Shaded horizontal gradient magnetic field (nanoteslas per meter) map of the same area shown in Figure 12A. Extent of map is shown on Figure 10. Base maps from the ArcGIS online map server (Esri, 2022).

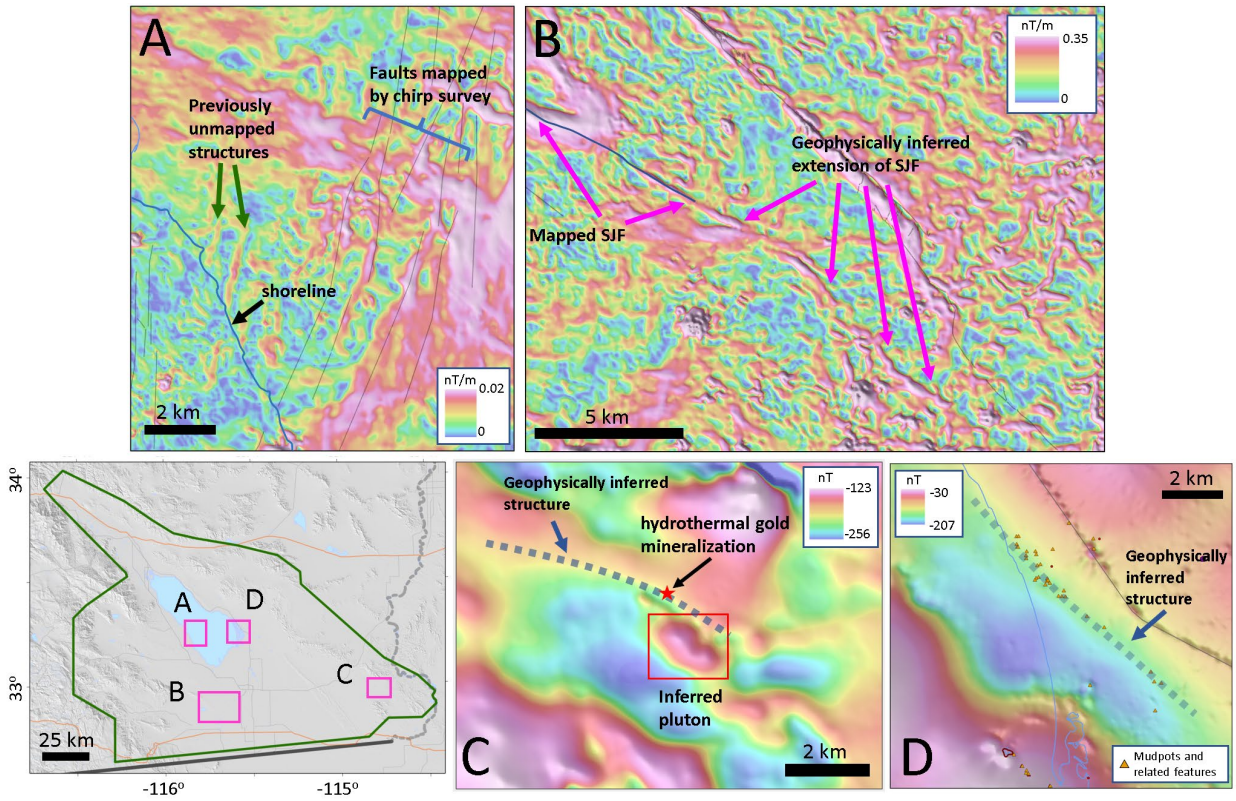

Figure 13. Lower left) Index map showing the locations of Figures 13 A-D that show results from the GeoFlight aeromagnetic survey. A) Shaded horizontal gradient magnetic field map showing magnetic signature of offshore structures inferred from seismic data. B) Shaded horizontal gradient magnetic field map depicting the geophysical signature of the San Jacinto Fault (SJF). C) Shaded TMI map of GeoFlight data over the Cargo Muchacho Mountains showing the location of hydrothermal gold mineralization and a geophysically-inferred fault from the aeromagnetic data. D) Shaded TMI map of GeoFlight data over the southern Salton Sea and SSGF showing the coincidence of hydrothermal features (mudpots and related features after Lynch and Hudnut, 2008), and a fault inferred from the new magnetic data. Base maps from the ArcGIS online map server (Esri, 2022).

4. Auxiliary Data

A key element of the EarthMRI program is the coordinated collection of detailed geologic mapping and high resolution lidar. In addition, ongoing efforts, conducted under the USGS Energy Resources Program and various GTO initiatives, support additional data collections and compilations that will complement the GeoDAWN and GeoFlight surveys.

4.1 Geologic mapping

Detailed geologic mapping was conducted by the State Geological Surveys with support from the USGS's Earth Mapping Resources Initiative (EarthMRI). Mapping accomplished under this collaboration was performed over areas principally with critical mineral potential and priority areas of study determined by EarthMRI and State Geological Surveys. Mapping performed as part of GeoDAWN was conducted by the Nevada Bureau of Mines and Geology within Clayton Valley with the focus on lithium clay resources. Mapping performed as part of GeoDAWN was conducted

by the California Geological Survey across Cargo Muchacho and Chocolate Mountains with a broad focus on gold mineralization and potential lithium clay source rocks.

4.2 Lidar

Lidar surveys spanning both GeoDAWN and GeoFlight geophysical survey extents were conducted through coordination with the USGS's 3D Elevation Program (3DEP). The resulting dataset provides a three-dimensional point cloud, that can be processed to show only ground returns and can be interpolated to form a surface, or digital elevation models (DEM) that provides a high resolution topographic base important to most geologic and geophysical interpretations. Lidar datasets can be manipulated to produce "bare earth" maps in which vegetation can be removed digitally, providing unprecedented topographic detail of the ground surface that can be useful in mapping active fault scarps even when their expression is subtle or concealed in heavily vegetated areas (e.g., Sherrod et al., 2004). This is particularly relevant to geothermal resource studies, since active geothermal systems are typically associated with young faulting that promotes permeability (Hickman et al., 1998; Faulds et al., 2010).

4.3 Gravity

As part of ongoing research conducted under the USGS Energy Program's Geothermal Resources Investigations Project (GRIP)[9], new gravity data compilations (combining new and existing data) are being developed to generate high resolution gravity grids for northern Nevada and southern California spanning GeoDAWN and GeoFlight surveys. These data will supplement the GeoDAWN and GeoFlight efforts because enable detailed joint gravity and magnetic modeling. In addition, regional depth to basement gravity inversions will be developed for the two areas to resolve basin geometries.

4.4 Rock Property and Paleomagnetic Data

Rock-property (density [dry bulk, grain and saturated bulk densities] and magnetic [magnetic susceptibility and remanence]) and paleomagnetic (magnetic remanence) measurements are routinely collected in conjunction with potential field studies. Typically, magnetic susceptibility measurements are performed on outcrops in the field, hand samples are collected for density measurements that are performed in the laboratory, and oriented paleomagnetic cores (or sometimes hand samples, in cases where drilling is not permitted or practical) are extracted from outcrops in order to constrain potential field models and interpretations. Model rock properties are based on these measurements, which ideally span all the principal rock units within a study area. In lieu of this, data can be derived from regional databases (e.g., Ponce, 2021) containing measurements made on similar lithologies.

5. Conclusions

The USGS and DOE have collaborated to acquire framework geoscience data (geologic mapping, geophysical surveys, and lidar data) for the nation in areas with critical mineral and geothermal potential. This led to two surveys being conducted over northwestern Nevada (GeoDAWN) and southern California (GeoFlight) that involved the acquisition of high resolution aeromagnetic and

[9] https://www.usgs.gov/centers/gmeg/science/geothermal-resource-investigations-project

aeroradiometric data. Coordinated with the geophysical surveys were efforts to collect lidar data over a comparable area, as well as detailed geologic mapping that was performed through partnership with State Geological Surveys.

These surveys provide critical information on surface and subsurface geology and structure. In addition, they can be used in both regional and detailed local studies, and can be integrated with a wide range of other datasets (e.g., gravity and electrical data). The data will aid several ongoing USGS and DOE projects (e.g., aimed at characterizing substantial geothermal and mineral systems, understanding the factors controlling their occurrence, and improving future national resource assessments), and will benefit other activities from hazard (earthquake, volcano, landslide, environmental) and resource (water, mineral, energy) studies, to mapping and land management.

Efforts are presently underway to make these data publicly available through USGS publications and online data repositories. Related ongoing efforts involve merging GeoDAWN and GeoFlight surveys with existing data to produce new state compilations and developing various other compatible datasets that will complement the aeromagnetic and aeroradiometric surveys.

Acknowledgments

We thank Jacob DeAngelo, Maria Richards, Gabe Matson, and Jeff Witter for constructive reviews of this manuscript. Ben Drenth provided much appreciated support during planning stages of the geophysical surveys. We thank Warren Day and Michael Weathers for their help sheepherding the USGS-DOE collaboration under which these surveys were conducted. Michael Hobbs graciously assisted with technical support. Any use of trade, firm, or product names is for descriptive purposes only and does not imply endorsement by the U.S. Government. This work was funded with support from the Department of Energy, Geothermal Technologies Office, and the U.S. Geological Survey Earth Mapping Resource Initiative and the Energy Resources Program.

REFERENCES

Airo, M.L. “Aeromagnetic And Aeroradiometric Response to Hydrothermal Alteration.”, *Surveys in Geophysics*, 23, (2002), 273–302.

Bankey, V. A., Cuevas, D., Daniels, A. A., and Finn, I. , Hernandez, I., Hill, P.L., Kucks, R., Miles, W., Pilkington, M., Roberts, C., Roest, W., Rystrom, V., Shearer, S., Snyder, S.L., Sweeney, R.E., and Velez, J. “Magnetic Anomaly Map of North America.”, *U.S. Geological Survey Special Map, (2002)*, https://doi.org/10.3133/70211067.

Blakely, R.J. “Potential Theory in Gravity and Magnetic Applications.” *Cambridge University Press*, New York, (1995), 441 p.

Blakely, R.J., and Simpson, R.W. “Approximating Edges of Source Bodies From Gravity or Magnetic Data.” *Geophysics*, 51, (1986), 1494–1498, doi: 10.1190/1.1442197.

Bouligand, C., Glen, J.M.G., and Blakely, R.J., “Distribution of Buried Hydrothermal Alteration Deduced From High-Resolution Magnetic Surveys in Yellowstone National Park.”, *J. Geophys. Res. Solid Earth*, 119, (2014), 2595–2630. Doi:10.1002/2013JB010802.

Bradley, D.C., Stillings, L.L., Jaskula, B.W., Munk, LeeAnn, and McCauley, A.D. "Lithium.", chap. K of Schulz, K.J., DeYoung, J.H., Jr., Seal, R.R., II, and Bradley, D.C., eds., "Critical mineral resources of the United States—Economic and environmental geology and prospects for future supply", *U.S. Geological Survey Professional Paper*, 1802, (2017), K1–K21, https://doi.org/10.3133/pp1802K.

Burns, E.R., and Glen, J.M.G. "The Path Forward: Updated and Brand-New National Geothermal Energy Assessments for the USA.", Geological Society of America, Abstracts with Programs, (2023).

Carmichael, R.S. "Magnetic Properties of Minerals and Rocks.", *in* Carmichael, R.S., ed., "CRC Handbook of Physical Properties of Rocks.", Boca Raton, Florida, *CRC Press, Inc.*, vol. 2, ch. 2, 229–287, (1982).

Clark, D.A. "Magnetic Petrophysics and Magnetic Petrology: Aids to Geological Interpretation of Magnetic Surveys", *AGSO Journal of Australian Geology & Geophysics*, 17(2), (1997), 83-103.

Cordell, L., and McCafferty, A.E. "A Terracing Operator for Physical Property Mapping With Potential Field Data." *Geophysics*, 54, (1989), 621–634. doi:10.1190/1.1442689.

Crafford, A.E.J. "Geologic Map of Nevada: U*.S.*", *Geological Survey Data Series,* 249, (2007). http://pubs.usgs.gov/ds/2007/249/.

Drenth, B.J., Grauch, V.J.S. "Finding the Gaps in America's Magnetic Maps.", *Eos*, 100, (2019), https://doi.org/10.1029/2019EO120449.

Duval, J.S. "Composite Color Images of Aerial Gamma-Ray Spectrometric Data.", *Geophysics*, 48(6), (1983). DOI:10.1190/1.1441502.

Duval, J.S. "Radioactivity and Some of its Applications in Geology.", *Proceedings of the Symposium on the Application of geophysics to Engineering and Environmental Problems*, *SAGEEP 89*, (1989), March 13-16, Golden, Colorado, p. 1-61.

Earney, T.E., Glen, J.M., Dean, B.J., Zielinski, L.A., Schermerhorn, W.D., Siler, D.L. "Characterizing Structure and Geology with Potential Field Geophysics to Assess Geothermal Potential Near Battle Mountain, NV.", *Geothermal Rising Conference,* (2022).

Faulds, J.E., Coolbaugh, M.F., Bouchot, V., Moek, I., and Oguz, K. "Characterizing Structural Controls of Geothermal Reservoirs in the Great Basin, USA, and Western Turkey: Developing Successful Exploration Strategies in Extended Terranes.", *Proceedings World Geothermal Congress*, (2010), 11 p., Bali, Indonesia.

Faulds, J.E., Hinz, N., Kreemer, C., Coolbaugh "Regional Patterns of Geothermal Activity in the Great Basin Region, Western USA: Correlation With Strain Rates.", *GRC Transactions*, 36 (2012), 897-902.

Faulds, J.E., Hinz, N., Coolbaugh, M., Ayling, B., Glen, J., Craig, J., McConville, E., Siler, D., Queen, J., Witter, J., and Hardwick, C. "Discovering Blind Geothermal Systems in the Great Basin Region: An Integrated Geologic and Geophysical Approach for Establishing Geothermal Play Fairways. Final Technical Report for Phases 1-3 (DE-EE0006731)." *Department of Energy* Technical Report, (2021), 73 p.

Faulds, J.E., and Henry, C.D. “Tectonic Influences on the Spatial and Temporal Evolution of the Walker Lane: An Incipient Transform Fault Along the Evolving Pacific – North American Plate Boundary.”, *in* Spencer, J.E., and Titley, S.R., eds. “Ores and Orogenesis: Circum-Pacific Tectonics, Geologic Evolution, and Ore Deposits.”, *Arizona Geological Society Digest*, 22, (2008), p. 437-470.

Glen, J.M.G, Earney, T.E., Zielinski, L.A., Schermerhorn, W.D., Dean, B.J., and Hardwick, C. “Regional Geophysical Maps of the Great Basin, USA.”, *U.S. Geological Survey data release*, (2022). https://doi.org/10.5066/P9Z6SA1Z.

Glen, J.M.G., McKee, E. H., Ludington, S., Ponce, D.A., Hildenbrand, T.G., and Hopkins, M.J. “Geophysical Terranes of the Great Basin and Parts of Surrounding Provinces.”, *U.S. Geological Survey Open-File Report*, 2004-1008, (2004), 303p.

Glen, J.M.G., and Ponce, D.A. “Large-scale Fractures Related to Inception of the Yellowstone Hotspot.”, *Geology*, 30/7, (2002), 647–650. doi: 10.1130/0091-7613(2002)030<0647:LSFRTI>2.0.CO;2.

Grauch, V.J.S., and Cordell, L. “Limitations of Determining Density or Magnetic Boundaries From the Horizontal Gradient of Gravity or Pseudogravity Data.” *Geophysics*, (1987), 118–121. doi: 10.1190/1.1442236.

Hickman S., Zoback, M., and Benoit, R. “Tectonic Controls on Reservoir Permeability in the Dixie Valley, Nevada Geothermal Field.”, *Proceedings: Twenty-third Workshop on Geothermal Reservoir Engineering, Stanford University*, January 26-28, (1998), 6 p.

Hoover, D.B., Reran, W.D., and Hill, P.L. “The Geophysical Expression of Selected Mineral Deposit Models.”, *U.S. Geological Survey Open-File report* 92-557, (1992), 129 p.

Hulen, J.B., Kaspereit, D., Norton, D.L., Osborn, W., and Pulka, F.S. “Refined Conceptual Modeling and a New Resource Estimate for the Salton Sea Geothermal Field, Imperial Valley, California.”, *GRC Transactions*, 36, (2002), 29-36.

Erdi-Krausz, G., Matolin, M. & Minty, B., Nicolet, J.P., Schetselaar, E. “Guidelines for Radioelement Mapping Using Gamma Ray Spectrometry Data.”, *IAEA*, Vienna, (2003). 173p.

Johnson, D.A., and Barton, M.D. “Guide for Field Trip Day 4: Buena Vista Hills, Humboldt Mafic Complex, Western Nevada.”, *in* Dilles, J. H., Barton, M. D., Johnson, D. A., Proffett, J. M., and Einaudi, M. T., eds., “Contrasting Styles of Intrusion Associated Hydrothermal Systems.”, *Society of Economic Geologists Guide Book Series*, 32, (2000), 145-162.

Kucks, R.P., Hill, P.L., and Ponce, D.A. “Nevada Magnetic and Gravity Maps and Data: A Website for the Distribution of Data.” *U.S. Geological Survey Data Series*, 234, (2006), http://pubs.usgs.gov/ds/2006/234.

Lynch, D.K., and Hudnut, K.W. “The Wister Mud Pot Lineament: Southeastward Extension or Abandoned Strand of the San Andreas Fault?”, *Bulletin of the Seismological Society of America*, 98(4,) (2008), 1720–1729, doi: 10.1785/0120070252.

Maden, N., Akaryalı, E. “Gamma Ray Spectrometry for Recognition of Hydrothermal Alteration Zones Related to a Low Sulfidation Epithermal Gold Mineralization (Eastern Pontides, NE Türkiye).”, *Journal of Applied Geophysics*, 122, (2015), 74-85.

McKibben, M.A., Elders, W.A., Raju, A.S.K. “Lithium and Other Geothermal Mineral and Energy Resources Beneath the Salton Sea.” *in* “Crisis At The Salton Sea: The Vital Role of Science.”, University of California, Riverside, (2021), 74-85.

Ponce, D.A. “Density and Magnetic Properties of Selected Rock Samples From the Western U.S. and Alaska.” *U.S. Geological Survey data release*, (2021). https://doi.org/10.5066/P9FONTGS.

Ponce, D.A., and Glen, J.M.G. “Relationship of Epithermal Gold Deposits to Large Scale Fractures in Northern Nevada.”, *Economic Geology*, 97(1), (2002), 3–9. https://doi.org/10.2113/gsecongeo.97.1.3.

Ponce, D.A., and Glen, J.M.G. “A Prominent Basement Feature Along the Northern Nevada Rift and its Geologic Implications, North-Central Nevada.”, *Geosphere*, 4(1) (2008), 207-217. https://doi.org/10.1130/GES00117.1.

Sherrod, B.L., Brocher, T.M., Weaver, C.S., Bucknam, R.C., Blakely, R.J., Kelsey, H.M., Nelson, A.R., and Haugerud, R. “Holocene Fault Scarps Near Tacoma, Washington, USA.”, *Geology*, 32, (2004), 9-12.